

Synthesis and coordination properties of new macrocyclic ligands: equilibrium studies and crystal structures

Gianluca Ambrosi,^a Paolo Dapporto,^b Mauro Formica,^a Vieri Fusi,^{*a} Luca Giorgi,^a Annalisa Guerri,^b Mauro Micheloni,^{*a} Paola Paoli,^b Roberto Pontellini^a and Patrizia Rossi^b

^a Institute of Chemical Sciences, University of Urbino, P.zza Rinascimento 6, I-61029, Urbino, Italy. E-mail: mauro@uniurb.it; Fax: +39-0722-350032; Tel: +39-0722-350032

^b Department of Energy Engineering, University of Florence, via S. Marta 3, I-50139, Florence, Italy

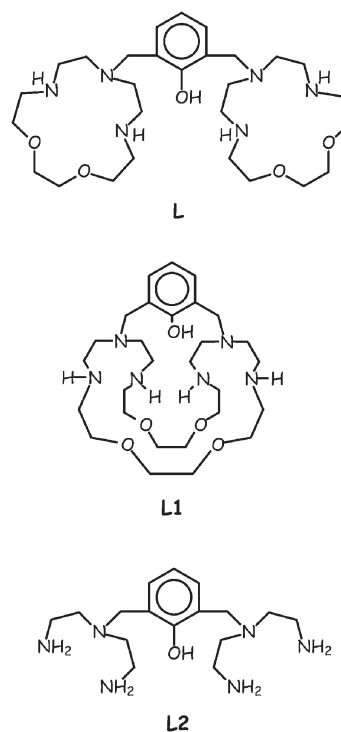
Received 10th June 2004, Accepted 2nd September 2004

First published as an Advance Article on the web 17th September 2004

The synthesis and characterization of two new macrocyclic ligands, the bis-macrocyclic compound 2,6-bis(1,4,13-triaza-7,10-dioxacyclopentadec-1-ylmethyl)phenol (**L**) and 38-methoxy-1,4,13,16,19,28-hexaaza-7,10,22,25-tetraoxatricyclo[14.14.7.1^{32,36}]octatrica-32,34,Δ^{36,38}-triene (**L1**) are reported. Equilibrium studies of basicity and coordination properties toward metal ions such as Cu(II), Zn(II), Cd(II) and Pb(II) were performed for ligand **L** by potentiometric measurements in aqueous solution (298.1 ± 0.1 K, *I* = 0.15 mol dm⁻³). **L** behaves as a hexaprotic base (log*K*₁ = 10.93, log*K*₂ = 9.70, log*K*₃ = 8.79, log*K*₄ = 8.05, log*K*₅ = 6.83, log*K*₆ = 2.55). All metal ions form stable mono- and dinuclear complexes: log*K*_{MLH₃} = 25.61 for Cu(II), 15.37 for Zn(II), 12.58 for Cd(II) and 13.79 for Pb(II); log*K*_{M₂LH₃} = 31.61 for Cu(II), 23.38 for Zn(II), 24.49 for Cd(II) and 23.68 for Pb(II). All these dinuclear species show a great tendency to add the OH⁻ group: the equilibrium constant for the addition reaction was found to be log*K*_{M₂LH₃OH} = 4.77 for Cu(II), 5.66 for Zn(II), 2.8 for Cd(II) and 3.18 for Pb(II). In the case of Ni(II), kinetic inertness prevents the possibility of solution studies. The dinuclear solid adducts [Ni₂H₋₁L(N₃)₃]·EtOH and [Cu₂H₋₁L(N₃)](ClO₄)₂ were characterized by X-ray analysis.

Introduction

The chemistry research community has always shown great interest in transition dinuclear metal complexes and ligands capable of yielding them due to the key role they play in many synthetic and biological applications. In fact, dinuclear metal complexes have been used successfully for the recognition and assembly of external species of different nature, including inorganic and organic substrates.¹⁻⁵ Many hydrolytic metallo-enzymes contain two divalent transition metal ions in close proximity which together form their active site.⁶⁻⁹ For example, urease catalyzes the hydrolysis of urea and small amine substrates around a dinuclear Ni(II) center,¹⁰ while alkaline phosphatase has Zn(II) as divalent ion,¹¹ and tyrosinase is a monooxygenase enzyme that has a dinuclear copper active site and is responsible for the hydroxylation of substrates.¹² In these systems, the distance between the two metals is crucial to allow the cooperation of both metal ions in the active center: for example, in hemocyanins 3.7 Å is the distance between the two copper ions necessary to allow binding and transport of dioxygen in the hemolymph of mollusks.¹³ Recently, we published results on transition dinuclear metal complexes formed with the ligand **L2** which are able to bind small molecules such as dioxygen, nitric oxide and others¹⁴ (see Scheme 1). These dinuclear complexes are characterized by metals close to each other and thus able to cooperate and bind a new species which is coordinated in a bridged disposition between the two metal centers. With the aim of synthesizing ligands able to bind two transition metal ions, we have now synthesized a new macrocyclic ligand 2,6-bis(1,4,13-triaza-7,10-dioxacyclopentadec-1-ylmethyl)phenol (hereafter abbreviated as (**L**)) showing two macrocyclic sub-units ([15]aneN₃O₂) spaced by a phenolic function and preserving the same binding skeleton as **L2**. This synthesis led to the isolation and characterization of **L1** (see Scheme 1), an isomeric ligand of **L** obtained in a very low yield. Ligand **L** can bind transition metal ions, forming dinuclear complexes in which the two metals are in close proximity. The two coordinated metals show an unsaturated coordination environment and thus can be used as receptors for secondary ligands.



Scheme 1 Schematic drawings of **L**, **L1** and **L2** ligands.

Results and discussion

Ligand preparation

Fig. 1 reports the synthetic pathway used to obtain compound 2,6-bis(1,4,13-triaza-7,10-dioxacyclopentadec-1-ylmethyl)phenol (**L**) and 38-methoxy-1,4,13,16,19,28-hexaaza-7,10,22,25-tetraoxatricyclo[14.14.7.1^{32,36}]octatrica-32,34,Δ^{36,38}-triene (**L1**). The scheme also provides the previous synthesis pathway for the tetraosylated compound **2**, which was synthesized in good yield by reacting **1** with tosyl chloride in chloroform in

the presence of a base. Compound **2** is a versatile building block that can be used to structure the coordination pattern of **L2**. In fact, starting from **2**, it is possible to link its four tosylamide groups by means of a cyclization reaction and thus produce different macrocyclic ligands. The properties of the ligands obtained can be varied by choosing suitable reactants. In this case, a derivative of a simple polyethylene glycol (**3**) was chosen as cyclization reagent. Although many other phenolic bridged ligands have been reported, the aim of the present work was to stiffen the molecular skeleton of **L2** without inserting other strong binding groups. Moreover, given the several binding sites in **2**, we wanted to determine the most favourable closing cyclization of **2** using a short and flexible reactant. In fact, in the most critical cyclization step (see Fig. 1) two main products are formed (**4** and **5**): the main compound (**5**) is obtained in 25% yield with the following two cyclizations, one involving the two tosyl amide groups of one of the triamine subunits and one on the other triamine subunit, forming two separate fifteen-membered [15]aneN₃O₂ macrocycles. Product **4**, which gave a significant lower yield (5%), arises from two cyclization reactions which link two tosylamide groups belonging to different triamine subunits. This new compound is formed by a single large thirty-membered [30]aneN₆O₄ macrocycle with two opposite nitrogen atoms bridged by the phenolic group and can thus be considered a large cryptand.

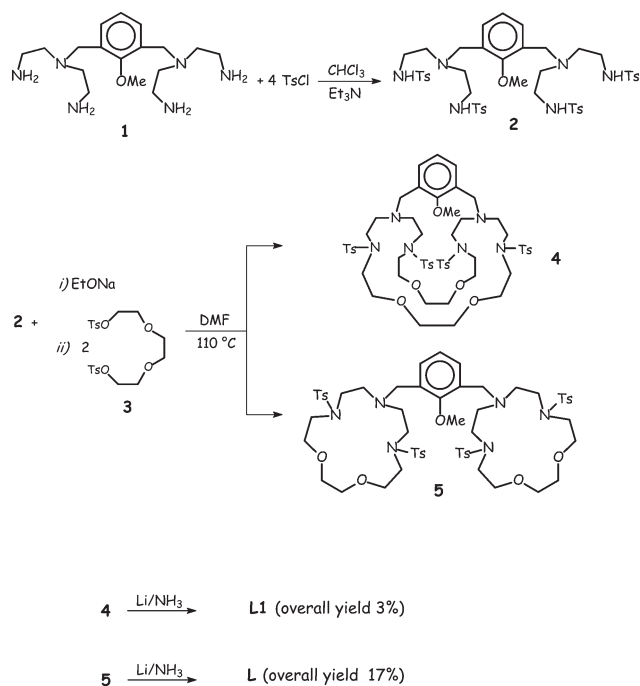


Fig. 1 Synthetic pathway used to obtain compounds **L** and **L1**.

The final ligands **L** and **L1** were obtained by simultaneous deprotection of the four tosyl and one methyl phenolic groups in lithium–liquid ammonia, following a standard procedure. The overall yields for the synthesis of **L** and **L1** were 17 and 3%, respectively. Compounds **L** and **L1** gave similar ¹H and ¹³C NMR spectra showing the same symmetry mediated on the NMR time scale and elemental analyses gave identical results; thus, the attribution of their molecular structure was very complicated. In the case of **L** this was done by solving the crystal structure, while for **L1** the molecular structure was inferred as shown in Scheme 1.

This structure was attributed taking into account the possible cyclization and above all the ESI mass spectra which showed the same molecular peak for both compounds. The molecular structure of **L1** was also validated by the product obtained following a standard deprotection of the tosyl groups with an HBr–AcOH mixture.^{14a} In this case, the main product obtained was the thirty-membered [30]aneN₆O₄ macrocycle derived from **4** by removing

Table 1 Protonation constants (log*K*) of **L** in H₂O at 298.15 K, *I* = 0.15 mol dm⁻³ NaCl

Reaction	log <i>K</i>
H _{−1} L [−] + H ⁺ = L	10.93(1) ^a
L + H ⁺ = LH ⁺	9.70(1)
LH ⁺ + H ⁺ = LH ₂ ²⁺	8.79(2)
LH ₂ ²⁺ + H ⁺ = LH ₃ ³⁺	8.05(1)
LH ₃ ³⁺ + H ⁺ = LH ₄ ⁴⁺	6.83(1)
LH ₄ ⁴⁺ + H ⁺ = LH ₅ ⁵⁺	2.55(2)

^a Values in parentheses are the standard deviations on the last significant figure.

all the aromatic groups. A similar procedure carried out with **5** led to the fifteen-membered [15]aneN₃O₂ macrocycle.

Equilibrium studies

Basicity. Table 1 summarizes the basicity constants of **L** as potentiometrically determined in 0.15 mol dm⁻³ NaCl aqueous solution at 298.1 K. Under the experimental conditions used, the neutral compound **L** behaves as monoprotic acid and as a pentaprotic base, although it has a total seven protonation sites. As shown in Table 1, **L** can be present in solution as anionic species H_{−1}L[−], and the stepwise basicity constants are reported starting from this species. The sequence of basicity constants of **L** can be easily explained in terms of positive charge repulsions. It is interesting to compare the basicity behavior of **L** with that of the related non-cyclic molecule 2,6-bis([bis(2-aminoethyl)-amino]methyl)phenol **L2**.^{14a} The latter molecule cannot be completely deprotonated under the usual experimental conditions because it is too strong base. Spectroscopic studies allowed the explanation of this basicity strength in terms of charge delocalization among phenolic oxygen and nitrogen atoms present in the lateral chains. In **L** the lateral chains containing the nitrogen atoms are portions of two macrocyclic frames of [15]aneN₃O₂; thus, the primary nitrogen atoms become secondary and the overall molecular framework less flexible; these conditions of reduced flexibility and the different set of donor atoms make **L** less basic than **L2**.

Coordination of metal ions. Table 2 reports the formation constants of different metal ions as potentiometrically determined in 0.15 mol dm⁻³ NaCl aqueous solution at 298.1 K. The symmetric molecular topology of **L** with two macrocyclic subunits linked by phenolic group is ideal for the formation of dinuclear complexes: **L** forms stable dinuclear complexes with all of the metal ions investigated, with the phenolate group bridging the two metal ions, and allows them to be close to each other in a coordination environment which is still unsaturated. Indeed, for Cu(II), Zn(II) and Pb(II) the dinuclear species M₂H_{−1}L³⁺ shows a great tendency to add the OH[−] group and form dinuclear hydroxo species such as [M₂H_{−1}L(OH)]²⁺. The involvement of the phenolate oxygen atom in the stabilization *via* a bridging disposition of both metal ions was confirmed by UV-Vis studies in the case of the **L**/Cu(II) system. The UV electronic spectrum, recorded in aqueous solution at the pH value where the [Cu₂(H_{−1}L)]³⁺ species is prevalent in solution, shows four principal bands: λ_{max} 242 (sharp, ε = 11200), 276 (sharp, ε = 8400), 374 (sharp, ε = 450) and 710 nm (large, ε = 200 dm³ cm⁻¹ mol⁻¹). The two bands at higher energy are due to the π–π* transitions of the phenolate group engaged in the coordination of the metals;¹⁵ the band at 374 nm can be ascribed to the phenolate–copper charge transfer when the oxygen atom bridges two Cu(II) ions,¹⁵ while the large band with λ_{max} 710 nm is due to the d–d electron transfer of the metal. These data indicate the involvement of the oxygen of the aromatic chromophore as phenolate in the stabilization of the complex and, moreover, that it bridges the two metals in the dinuclear species. However, **L** also forms mononuclear species with the four M(II) ions

Table 2 Formation constants ($\log K$) of **L** with Cu(II), Zn(II), Cd(II) and Pb(II) ions in H₂O at 298.15 K, $I = 0.15 \text{ mol dm}^{-3}$ NaCl

Reaction	M = Cu	M = Zn	M = Cd	M = Pb
$M^{2+} + H_{-1}L^- = MH_{-1}L^+$	25.61(2) ^a	15.37(1)	12.58(1)	13.79(1)
$M^{2+} + L = ML^{2+}$	21.17(1)	13.53(1)	11.16(1)	11.49(1)
$MH_{-1}L^+ + H^+ = ML^{2+}$	6.84(1)	9.44(2)	9.85(2)	9.32(1)
$ML^{2+} + H^+ = MHL^{3+}$	4.35(1)	8.45(1)	8.37(1)	8.43(2)
$MHL^{3+} + H^+ = MH_2L^{4+}$	3.65(2)	—	—	—
$MH_2L^{4+} + H^+ = MH_3L^{5+}$	3.55(1)	—	—	—
$MH_{-1}L^+ + OH^- = MH_{-1}L(OH)$	3.07(1)	—	—	—
$MH_{-1}L^+ + M^{2+} = M_2H_{-1}L^{3+}$	6.00(1)	8.01(1)	11.91(1)	9.89(1)
$M_2H_{-1}L^{3+} + OH^- = M_2H_{-1}L(OH)^{2+}$	4.77(3)	5.66(3)	2.8(1)	3.18(2)
$M_2H_{-1}L(OH)^{2+} + OH^- = M_2H_{-1}L(OH)_2^+$	—	2.72(2)	—	—

^a Values in parentheses are the standard deviations on the last significant figure.

examined. The binding constant for the Cu(II) complex is very large: 21.17 log units, as reported in Table 2. This value is however comparable with the binding constant for the related macrocycle [15]aneN₃O₂: $\log K = 15.51$ as already reported.¹⁶ The difference can be explained by taking into consideration that in the case of **L** there is one extra phenolic oxygen as donor atom. The mononuclear species are the most prevalent in solution when using a ligand:metal molar ratio of 1:1; when the **L**/M(II) molar ratio is lower, dinuclear species become prevalent and are almost the only species present in solution at a ligand:metal molar ratio of 1:2. This behavior is depicted, for example, in Fig. 2(a) and (b), which show the distribution diagrams for these species for the system **L**/Zn(II), at 1:1 and 1:2 molar ratios respectively, as a function of pH. All of the $[MH_{-1}L]^+$ mononuclear species undergo at least two easy protonations, suggesting, as in the case of **L2**, that only one macrocyclic subunit is strongly involved in the coordination of a M(II) ion while the other unit remains available for protonation.

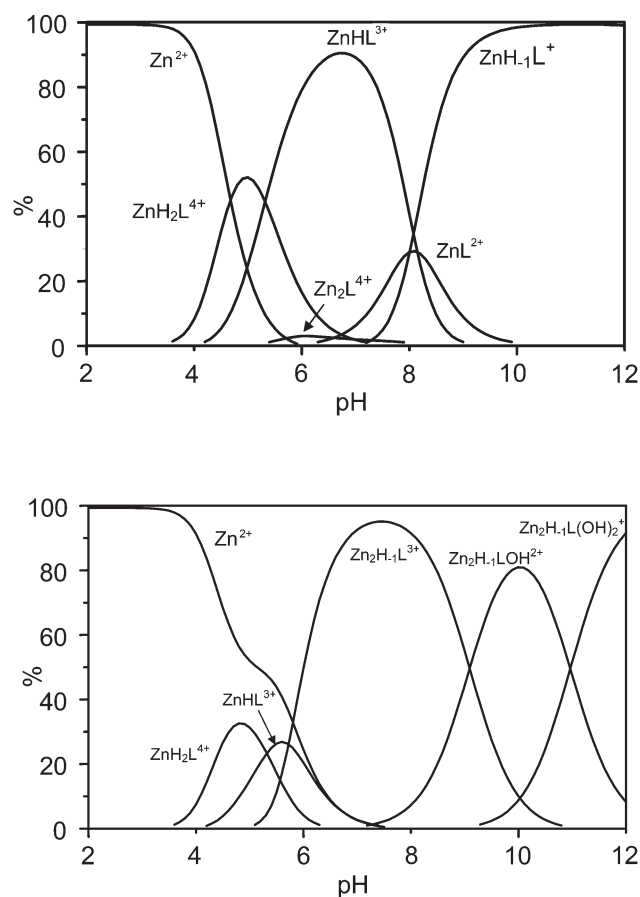


Fig. 2 Distribution diagrams of the species for the system **L**/Zn(II) as a function of pH in aqueous solution, $I = 0.15 \text{ mol dm}^{-3}$ NaCl, at 298.1 K. (a) $[L] = 1 \times 10^{-3} \text{ mol dm}^{-3}$, $[Zn^{2+}] = 1 \times 10^{-3} \text{ mol dm}^{-3}$; (b) $[L] = 1 \times 10^{-3} \text{ mol dm}^{-3}$, $[Zn^{2+}] = 2 \times 10^{-3} \text{ mol dm}^{-3}$.

Upon comparison of the stability of the complexes formed with **L** and **L2**, it is possible to note that the Cu(II) and Zn(II) complexes formed with **L** are significantly less stable than those found with **L2**^{14a,d} (see Table 2). This clearly indicates that the presence of the bulky oxygen containing macrocycles makes the overall molecular framework less flexible and adaptable to the metal ion coordination requirement; moreover, the oxygen atoms introduced do not participate in stabilizing the metal ions. On the contrary, the Pb(II) dinuclear complexes show a significantly higher stability, leading us to suppose that in the case of harder metal ions, the oxygen atoms of the [15]aneN₃O₂ subunits contribute to stabilize the species.

X-Ray crystal structures

In $[Ni_2(H_{-1}L)(N_3)_3] \cdot EtOH$ (**6**) the asymmetric unit contains half of the dinuclear complex, one and a half azide anions and a disordered molecule of ethanol to which a population parameter of 0.5 was assigned. The two halves of the metal complex are related by a two-fold symmetry axis which passes through an azide anion, namely N(7)–N(8)–N(9) and the O(1), C(1), C(4) and H(4) atoms of the ligand (Fig. 3). In the crystal structure of $[Cu_2(H_{-1}L)(N_3)](ClO_4)_2$ (**7**) the asymmetric unit is made up of one molecule of the dinuclear complex, an azide ion and two perchlorate anions (Fig. 4).

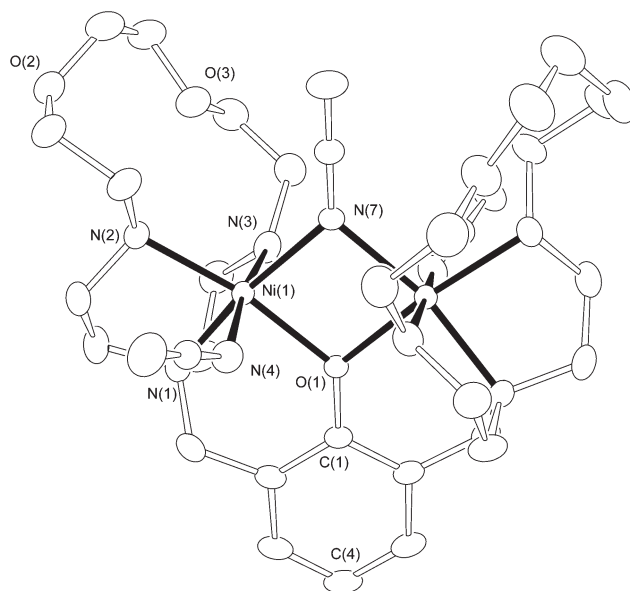


Fig. 3 ORTEP view of the dinuclear Ni(II) complex **6**. For the sake of clarity only the independent atoms have been labelled. Ellipsoids are drawn at 30% probability.

The way in which the $H_{-1}L^-$ species is wrapped around the metal ions filling, albeit only partially, their coordination sites is almost identical in both the metal complexes, *i.e.* it provides four donor atoms for each cation, namely N(1), N(2), N(3) and

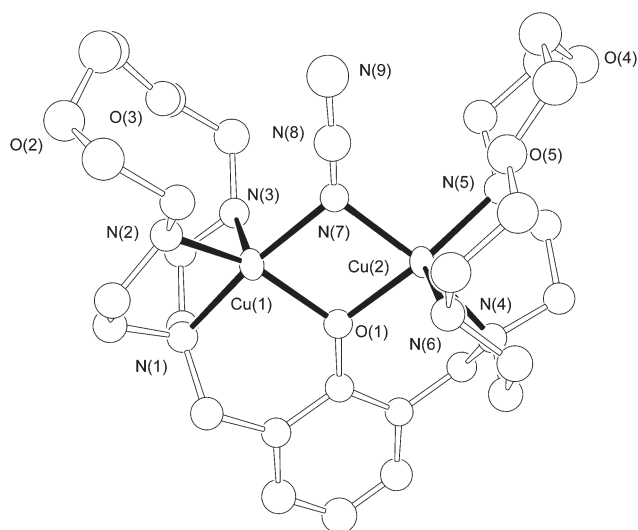


Fig. 4 ORTEP view of the dinuclear Cu(II) complex **7**. Ellipsoids are drawn at 30% probability.

the phenyl oxygen atom O(1). In both structures the latter acts as bridging unit between the two metal ions, keeping the Ni(II) and the Cu(II) ions in close proximity (3.150(7) and 3.118(3) Å, respectively). The restricted number of donors (four) supplied by the ligand to each metal ion and the closeness of the two metal cations enable the latter to assemble and share external species in order to complete their coordination sphere, as already reported on ligands featuring a coordination pattern similar to that provided by **L**. In those cases the two metal ions worked together to recognize external guests such as chloride, hydroxide, azide, and butanolate anions.^{14a-c} In the present paper the M–M distances, which are in the expected range for Ni(II) and Cu(II) binuclear complexes featuring analogous bridging units,¹⁷ well suit the recognition and the assembly of the azide anion, in which the nitrogen atom N(7) further links the two metal ions.

In the crystal structure of **6** each nickel ion completes its coordination sphere, which can be described as an elongated octahedron, thanks to N(4) which belongs to another azide ion. The Ni–donor atom bond distances are in the range usually observed for analogous Ni(II) complexes as provided by a search in the Cambridge Structural Database (CSD) v. 5.25,¹⁷ with the Ni(1)–N(3) (2.164(2) Å) and Ni(1)–N(4) (2.168(3) Å) distances significantly longer than the Ni–N equatorial bonds (mean value 2.08 Å). The atoms O(1), N(1), N(2) and N(7) lie well in a plane and the metal ion is displaced from it only 0.0171(4) Å towards N(4).

In **7**, the coordination sphere (*vide infra*) described by the ligand and the bridging azide ion around the Cu(II) ions strictly resembles that of the dinuclear nickel complex **6**. Thus each copper ion has a square pyramidal coordination geometry (Fig. 4), with the Cu(II) ions slightly shifted towards the apical donors (the maximum displacement from the mean plane defining the base being that of Cu(1) (0.274(2) Å). All the Cu–donor atom distances are in agreement with those of analogous complexes found in the CSD, with, as expected, the bond lengths involving the apical donors longer with respect to the other Cu–N distances. Incidentally, for each Cu(II) ion, the sixth coordination site of the octahedron appears to be occupied by a perchlorate oxygen atom, even though the latter is definitely distant from the metal ions (>3.20 Å). This is also true for the already reported solid state structure of the copper binuclear complex with **L2** (*vide infra*).^{14b} The IR spectra show only asymmetric stretching of the azide at 2079 cm⁻¹ attributed to the μ -1,1-azido bridge between the two metal ions.¹⁸

The mean planes described by the equatorial donors in **7** form an angle of 19.3(3)° each other and of 12.5(3) and 14.6(3)° with the aromatic ring, respectively. In **6** the four equatorial donors are almost coplanar with respect to the phenol moiety (8.6(1)°).

In both the metal complexes the geometrical parameters of the azide anions are within the expected range.

Given that the [15]aneN₃O₂ macrocycle acts as a tridentate ligand through the nitrogen atoms, its binding skeleton strongly resembles that of **L2**. This similarity prompted us to compare the 3D arrangement of the phenol group and the polyamine side arms of **L**, as found in **6** and **7**, with the corresponding atoms of **L2** in the dinuclear complexes of Ni(II) and Cu(II), already reported^{14a} (hereafter denoted as Ni₂**L2** and Cu₂**L2**), and the latter metal ions were found to show a coordination environment that is very similar to that of the current complexes. The relative arrangement of the mean planes described by the equatorial donors and the phenol ring in **6**, **7**, Ni₂**L2** and Cu₂**L2** is also quite similar. The pronounced binding similarity between **L** and **L2** is also provided by the root mean square values obtained from the superimposition (Fig. 5) of the non-hydrogen atoms of the phenol group and the polyamine side arms: 0.46 for the **6**/Ni₂**L2** couple and 0.57 for the **7**/Cu₂**L2** pair.

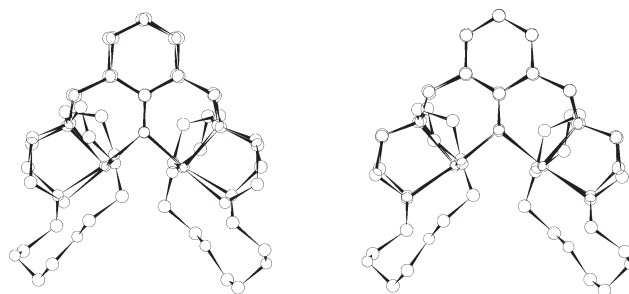


Fig. 5 Binding skeleton superimposition of the **7**/Cu₂**L2** (left) and **6**/Ni₂**L2** (right) couples.

Finally, in both species the macrocycles exhibit a quite complex conformation resulting from two different types of interactions. As already stated, while the region of the nitrogen donors is involved in the coordination of the metal ions, the non-coordinating oxygen atoms O(2) and O(3) in **6** and O(2), O(3), and O(4), O(5) in **7** are involved, as acceptors, in several intramolecular H-bonds. Particularly in **6**, N(2) is hydrogen bonded to O(2) and O(3); the distances are: 2.900(4) and 2.922(4) Å, respectively. In **7** the corresponding distances are 2.76(1) and 2.94(1) Å, and 2.81(1) and 2.97(1) Å for the interactions between the nitrogen atom N(5) and O(4) and O(5), respectively. Moreover, the nitrogen atom N(3) in **6** interacts with the symmetry-related N(4) atom reported by the operation $-x + 1, y, -z + 1/2 + 1$, the distance being 3.009(3) Å.

Conclusions

In order to synthesize the new ligands **L** and **L1** we first synthesized compound **2**, a suitable building block showing the coordination environment present in **L2**. During the cyclization step, two isomeric ligands **L1** and **L**, obtained in different yields, were isolated. The two ligands arise from two different cyclization schemes. **L1** is a large cryptand formed by a thirty-membered [30]aneN₆O₄ macrocycle with two opposite nitrogen atoms bridged by the phenolic group, while **L** contains two [15]aneN₃O₂ macrocyclic subunits linked by a 2,6 dimethylphenol unit. The coordination behavior of **L** towards several bivalent metal ions was investigated. **L** forms stable dinuclear complexes with Cu(II), Zn(II), Cd(II) and Pb(II) ions, in which the phenolate group bridging the two metal ions allows them to be close to each other in an unsaturated coordination environment. Solution studies highlighted the great tendency of the [M₂H₋₁L]³⁺ species to bind hydroxide, suggesting that the OH⁻ probably bridges the two metal centres. Kinetic inertness in the complex formation of the Ni(II)/**L** system prevented the evaluation of the stability constants. In any case, the crystal structures obtained confirm the tendency to add an extra ligand such as the azide anion to the dinuclear complexes. The coordination

features of the dinuclear complexes formed with **L** will permit their use in biological mimicking of active bimetallic centres and in molecular recognition of further substrates.

Experimental

General methods

^1H and ^{13}C NMR spectra were recorded with a Bruker AC-200 instrument, operating at 200.13 and 50.33 MHz, respectively. Peak positions are reported in relation to TMS (CDCl_3) or HOD at 4.75 ppm (D_2O). Dioxane was used as reference standard in ^{13}C NMR spectra (67.4 ppm). IR spectra were recorded with a Shimadzu FT-IR-8300 spectrometer. UV absorption spectra were recorded at 298 K with a Varian Cary-100 spectrophotometer equipped with a temperature control unit. ESI mass spectra were recorded with a ThermoQuest LCQ Duo LC/MS/MS spectrometer. All reagents and solvents used were of analytical grade.

Synthesis

The overall synthetic sequence used to obtain compounds **L** and **L1** is reported in Fig. 1. 2,6-bis{[bis(2-aminoethyl)amino]-methyl}anisole **1** was prepared as previously described;¹⁹ solvents and starting materials were used as purchased.

Synthesis of compound (L)

The overall synthetic sequence is reported in Fig. 1. Product **1** has already been reported in ref. 19. To prepare compound **2**, 10 g of **1** (0.018 mol) were dissolved in 150 cm^3 of CHCl_3 and placed in a round-bottom flask, to which 50 g of triethylamine were slowly added. 300 cm^3 of CHCl_3 containing 21 g of *p*-toluenesulfonyl chloride were added dropwise, under stirring, to the resulting solution. The reaction mixture was left at room temperature, under stirring, for at least 24 h, after which the solvent was evaporated under vacuum. The sticky oil obtained was dissolved in hot isopropanol and the resulting solution was left to cool overnight. The two phases were then separated: the solid phase was discharged while the liquid alcoholic phase was concentrated under vacuum, obtaining a white solid. The product was recrystallised from ethanol, yielding 11 g (69%). Elemental analysis: Anal. Calc. for $\text{C}_{45}\text{H}_{58}\text{N}_6\text{O}_9\text{S}_4$: C 56.58; H 6.12; N 8.80. Found: C 56.7; H 6.0; N 8.7%. ^1H NMR (CDCl_3 ; 200 MHz): δ 7.72 (d, 8H), 7.59 (d, 2H), 7.26 (d, 8H), 7.08 (t, 1H), 5.63 (br, 1H), 3.61 (s, 3H), 3.58 (s, 4H), 2.92 (t, 8H), 2.56 (t, 8H), 2.40 (s, 12H).

Preparation of compounds 38-methoxy-4,13,19,28-tetrakis(4-toluensulfonyl)-1,4,13,16,19,28-hexaaza-7,10,22,25-tetra-oxatricyclo[14.14.7.1^{32,36}]octatrica-32,34, Δ ^{36,38}-triene **4** and 2,6-bis[4,13-bis(4-toluensulfonyl)1,4,13-triaza-7,10-dioxacyclopentadec-1-ylmethyl]-1-methoxybenzene **5**

15.5 g of **2** (0.016 mol) and 80 cm^3 of dry ethanol, were mixed in a three-neck round-bottom flask, equipped with condenser, drying tube and nitrogen inlet. The solution was heated to reflux and then freshly made sodium ethanolate (1.7 g of **3** dissolved in 60 cm^3 of absolute ethanol) was quickly added. After a few min a white solid formed and the reaction mixture was left under stirring for 2 h. The solvent was removed from the reaction mixture by distillation under nitrogen, after which the resulting white sodium salt was dried under vacuum. The solid obtained was suspended in 500 cm^3 of dry DMF and the reaction mixture heated to 110 $^\circ\text{C}$. 14.9 g (0.032 mol) of tri(ethylene glycol) di-*p*-tosylate **3** (Aldrich Chemical) dissolved in 300 cm^3 of dry DMF were added dropwise to the previously stirred solution over a period of 6 h. The reaction mixture was left under reflux for a further 2 h, after which half of the solvent was slowly evaporated, and the solution obtained poured into a beaker containing a mixture of water and ice. The brownish solid which formed was filtered off, washed with water and dried

under vacuum. The crude product was chromatographed on neutral alumina (CH_2Cl_2 -MeOH, 100:0.2). The eluted fractions were collected and evaporated, affording **4** (4.5 g, 24%) and **5** (0.9 g, 4.8%) as white solids.

Compound 4. Anal. Calc. for $\text{C}_{57}\text{H}_{78}\text{N}_6\text{O}_{13}\text{S}_4$: C 57.85, H 6.64, N 7.10. Found: C 57.7, H 6.5, N 7.0%.

^1H NMR (CDCl_3): δ 7.84 (d, 2H), 7.70 (d, 8H), 7.30 (d, 8H), 7.23 (t, 1H), 3.67 (m, 7H), 3.60 (m, 8H), 3.49 (s, 8H), 3.36 (m, 8H), 3.27 (m, 16H), 2.43 (s, 12H).

^{13}C NMR (CDCl_3): δ 157.4, 143.6, 136.5, 132.6, 129.7, 127.0, 126.9, 123.8, 72.7, 70.5, 61.8, 53.7, 53.4, 49.7, 48.3, 21.5.

Compound 5. Anal. Calc. for $\text{C}_{57}\text{H}_{78}\text{N}_6\text{O}_{13}\text{S}_4$: C 57.85, H 6.64, N 7.10. Found: C 58.0, H 6.7, N 7.0%.

^1H NMR (CDCl_3): δ 7.64 (d, 2H), 7.49 (d, 8H), 7.26 (t, 1H), 7.15 (d, 8H), 3.67 (s, 4H), 3.74 (s, 3H), 3.59 (m, 8H), 3.53 (s, 8H), 3.26 (m, 16H), 2.63 (m, 8H), 2.31 (s, 12H).

^{13}C NMR (CDCl_3): δ 157.3, 143.1, 136.5, 132.6, 129.7, 129.4, 126.9, 123.8, 72.5, 70.5, 61.8, 53.7, 53.4, 49.6, 48.3, 21.4.

Compound L-6HBr

Ammonia (300 cm^3) was condensed in a suspension of **4** (4.5 g, 3.8 mmol) in diethyl ether (30 cm^3) and methanol (1 cm^3), cooled at -70 $^\circ\text{C}$. Small pieces of lithium were added to the mixture until the suspension turned blue. Thirty minutes after the suspension turned blue, NH_4Cl (12 g, 0.2 mol) was added. The white solid obtained after the evaporation of the solvents was treated with 3 mol dm^{-3} HCl (3 \times 100 cm^3). The acidic solution was filtered and then evaporated to dryness, after which the resulting solid was dissolved in the minimum amount of water necessary and the solution made alkaline with concentrated NaOH. The liquid was extracted with CHCl_3 (6 \times 50 cm^3). The organic layer was dried over Na_2SO_4 and vacuum-evaporated to obtain a solid that was dissolved in ethanol and treated with 48% HBr until complete precipitation of a white solid, which was filtered off to obtain **L** as a hexahydrobromide salt (2.9 g, 71%).

Anal. Calc. for $\text{C}_{28}\text{H}_{58}\text{Br}_6\text{N}_6\text{O}_5\cdot\text{H}_2\text{O}$: C 31.84, H 5.73, N 7.96; Found: C 32.0, H 5.6, N 7.7%. MS (ES): m/z 554 (M + H)⁺

^1H NMR (D_2O ; pH = 3): δ 7.28 (d, 2H), 6.97 (t, 1H), 3.93 (s, 4H), 3.71 (t, 8H), 3.64 (s, 8H), 3.26 (t, 8H), 3.17 (t, 8H), 3.02 (t, 8H).

^{13}C NMR (D_2O ; pH = 3): δ 155.0, 133.5, 124.4, 123.1, 70.9, 66.5, 55.3, 50.6, 47.6, 44.7.

Compound L1-6HBr

By treating compound **5** as already described for compound **4**, 0.53 g (73%) of the hexahydrobromide salt of **L1** were obtained.

Anal. Calc. for $\text{C}_{28}\text{H}_{58}\text{Br}_6\text{N}_6\text{O}_5\cdot 2\text{H}_2\text{O}$: C 31.31, H 5.82, N 7.82; Found: C 31.2, H 5.9, N 7.7%. MS (ES): m/z 554 (M + H)⁺

^1H NMR (D_2O ; pH = 3): δ 7.22 (d, 2H), 6.85 (t, 1H), 3.79 (s, 4H), 3.68 (t, 8H), 3.61 (s, 8H), 3.18 (t, 8H), 3.03 (m, 16H).

^{13}C NMR (D_2O ; pH = 3): δ 154.9, 133.8, 124.1, 123.0, 70.7, 67.3, 54.6, 51.1, 46.9, 44.3.

[Ni₂H₋₁L(N₃)₃] \cdot EtOH (**6**)

A sample of $\text{Ni}(\text{ClO}_4)_2\cdot 6\text{H}_2\text{O}$ (36.6 mg, 0.1 mmol) in ethanol (20 mL) was slowly added to an ethanolic solution (30 mL) of **L** (27.4 mg, 0.05 mmol). The resulting solution was stirred at room temperature for 10 min, after which NaN_3 (12.8 mg, 0.2 mmol) was added. The slow evaporation of the solvent led to crystallization of complex **6** as green crystals suitable for X-ray analysis.

[Cu₂H₋₁L(N₃)₃](ClO₄)₂ (**7**)

A sample of $\text{Cu}(\text{ClO}_4)_2\cdot 6\text{H}_2\text{O}$ (37.1 mg, 0.1 mmol) in ethanol (20 mL) was slowly added to an ethanolic solution (30 mL)

Table 3 Crystal data and refinement parameters for **6** and **7** (refinement method: full-matrix least-squares on F^2)

	6	7
Empirical formula	C ₃₀ H ₅₇ N ₁₅ Ni ₂ O ₆	C ₂₈ H ₅₁ N ₉ O ₁₃ Cu ₂ Cl ₂
<i>M</i>	841.33	919.76
<i>T</i> /K	298	298
λ /Å	1.54184	1.54184
Crystal system	Monoclinic	Orthorhombic
Space group	<i>C2/c</i>	<i>Pbca</i>
<i>a</i> /Å	24.077(1)	19.624(4)
<i>b</i> /Å	12.677(1)	19.449(4)
<i>c</i> /Å	13.632(1)	21.008(5)
β /°	112.576(5)	
<i>V</i> /Å ³	3842.0(4)	8018(3)
<i>Z</i> , <i>D</i> , g cm ⁻³	4, 1.455	8, 1.524
μ /mm ⁻¹	1.736	3.141
<i>F</i> (000)	1784	3824
Crystal size/mm	0.3 × 0.4 × 0.5	0.2 × 0.2 × 0.4
θ Range for data collection/°	3.98–64.14	3.83–58.01
Limiting indices, <i>hkl</i>	–28 to 1, –1 to 14, –14 to 15	–18 to 21, –20 to 20, –21 to 22
Reflections collected/unique	3706/3150	31699/5510
Data/parameters	2779/0/257	1837/0/238
Goodness-of-fit on F^2	1.081	0.905
Final <i>R</i> indices [<i>I</i> > 2 σ (<i>I</i>)]	<i>R</i> 1 = 0.0424, <i>wR</i> 2 = 0.1219	<i>R</i> 1 = 0.0989, <i>wR</i> 2 = 0.2352

of **L** (27.4 mg, 0.05 mmol). The resulting solution was stirred at room temperature for 10 min, after which NaN₃ (12.8 mg, 0.2 mmol) was added. The slow evaporation of the solvent led to crystallization of complex **7** as green crystals suitable for X-ray analysis.

EMF measurement

Equilibrium constants for **L** protonation and complexation reactions were measured by pH-metric methods (pH = $-\log[\text{H}^+]$) in 0.15 mol dm⁻³ NaCl at 298.15 ± 0.1 K using the fully automatic equipment that has already been described.²⁰ The EMF data were collected with the PASAT computer program.²¹ The combined glass electrode was calibrated as a hydrogen concentration probe by titrating known amounts of HCl with CO₂-free NaOH solutions and measuring the end point by Gran's method,²² which provides both the standard potential E° and the ionic product of water ($\text{p}K_w = 13.73(1)$ at 298.1 K in 0.15 mol dm⁻³ NaCl, $K_w = [\text{H}^+][\text{OH}^-]$). At least three potentiometric titrations were performed for each system in the pH range 2–11, using different molar ratio of M(n)/L ranging from 1:1 to 2:1. All titrations were treated either as single sets or as separate entities, for each system; no significant variations were found in the values of the determined equilibrium constants. The HYPERQUAD computer program was used to process all potentiometric data.²³

X-Ray crystallography

For compound [Ni₂(H₋₁L)(N₃)₃]·EtOH **6** intensity data were collected on a Siemens P4 four-circle diffractometer using graphite-monochromated Cu-K α radiation ($\lambda = 1.54184$ Å), $T = 298$ K. Data were corrected for Lorentz and polarization effects. Absorption correction was performed with the DIFABS²⁴ program.

Intensity data for compound [Cu₂(H₋₁L)(N₃)](ClO₄)₂ **7** were collected on a Siemens/Bruker diffractometer equipped with rotating anode and CCD area detector, using Cu-K α radiation ($\lambda = 1.54184$ Å), $T = 298$ K and the SMART program.²⁵ Six settings of ω were run and narrow data "frames" were collected for 0.3° increments in ω . A total of 3300 frames of data were stored, providing a sphere of data. Data reductions were performed with the SAINT 4.0 program.²⁶ Absorption corrections were performed with the program SADABS.²⁷

Both structures were solved by direct methods using the SIR97 program²⁸ and refined by full-matrix least squares against F^2 using all data (SHELX97²⁹).

Table 4 Selected bond lengths (Å) for compounds **6** and **7**

6		7	
Ni(1)–O(1)	2.054(2)	Cu(1)–O(1)	1.997(8)
Ni(1)–N(1)	2.084(2)	Cu(1)–N(1)	2.03(1)
Ni(1)–N(2)	2.084(2)	Cu(1)–N(2)	2.02(1)
Ni(1)–N(7)	2.093(2)	Cu(1)–N(7)	2.02(1)
Ni(1)–N(3)	2.164(2)	Cu(1)–N(3)	2.24(1)
Ni(1)–N(4)	2.168(3)		
		Cu(2)–O(1)	1.981(8)
		Cu(2)–N(4)	2.04(1)
		Cu(2)–N(5)	2.03(1)
		Cu(2)–N(7)	2.06(1)
		Cu(2)–N(6)	2.23(1)

For compound **6**, anisotropic thermal parameters were used for the non H-atoms while an overall isotropic thermal parameter was used for the hydrogen ones. The latter atoms were all introduced in calculated positions with the exception of the hydrogen atoms of the ethanol molecule, which were not set. The ethanol molecule is near an inversion center and a population factor of 0.5 was assigned to the O(4), C(16) and C(17) atoms.

Because of the poor observed reflections/parameters ratio, in compound **7** only the Cu and Cl atoms were refined anisotropically, while all the others were treated isotropically. The hydrogen atoms were set in calculated positions and refined with a thermal parameter depending on the atom to which they are bound.

Geometrical calculations were carried out by PARST97³⁰ and molecular plots were produced by the ORTEP3 program.³¹ Table 3 reports details of the crystal data, data collection, structure solution and refinement. Tables 4 and 5 list the bond distances and angles defining the metal environments.

CCDC reference numbers 235120 and 235121.

See <http://www.rsc.org/suppdata/dt/b4/b408808e/> for crystallographic data in CIF or other electronic format.

Acknowledgements

Financial support from the Italian Ministero dell'Università e della Ricerca Scientifica e Tecnologica (PRIN2002) and CRIST (Centro Interdipartimentale di Cristallografia Strutturale, where all the X-ray measurements were carried out) are gratefully acknowledged.

Table 5 Selected angles (°) for compounds **6** and **7**

6		7			
O(1)–Ni(1)–N(1)	89.75(9)	O(1)–Cu(1)–N(1)	93.2(4)	O(1)–Cu(2)–N(4)	91.5(4)
O(1)–Ni(1)–N(2)	169.72(8)	O(1)–Cu(1)–N(2)	151.2(4)	O(1)–Cu(2)–N(5)	153.7(4)
O(1)–Ni(1)–N(3)	90.09(7)	O(1)–Cu(1)–N(3)	99.5(3)	O(1)–Cu(2)–N(6)	97.2(4)
O(1)–Ni(1)–N(4)	82.68(7)				
O(1)–Ni(1)–N(7)	81.09(9)	O(1)–Cu(1)–N(7)	78.8(4)	O(1)–Cu(2)–N(7)	78.2(4)
N(1)–Ni(1)–N(2)	84.5(1)	N(1)–Cu(1)–N(2)	86.3(4)	N(4)–Cu(2)–N(5)	86.5(4)
N(1)–Ni(1)–N(3)	81.6(1)	N(1)–Cu(1)–N(3)	82.0(4)	N(4)–Cu(2)–N(6)	83.5(4)
N(1)–Ni(1)–N(4)	96.5(1)				
N(1)–Ni(1)–N(7)	165.58(9)	N(1)–Cu(1)–N(7)	171.7(4)	N(4)–Cu(2)–N(7)	169.6(4)
N(2)–Ni(1)–N(3)	97.4(1)	N(2)–Cu(1)–N(3)	108.9(4)	N(5)–Cu(2)–N(6)	108.6(4)
N(2)–Ni(1)–N(4)	89.5(1)				
N(2)–Ni(1)–N(7)	106.2(1)	N(2)–Cu(1)–N(7)	101.7(4)	N(5)–Cu(2)–N(7)	103.3(4)
N(3)–Ni(1)–N(4)	172.6(1)				
N(3)–Ni(1)–N(7)	87.27(7)	N(3)–Cu(1)–N(7)	97.0(4)	N(6)–Cu(2)–N(7)	96.2(4)
N(4)–Ni(1)–N(7)	93.34(8)				

References

- (a) C. J. Pedersen, *J. Am. Chem. Soc.*, 1967, **89**, 7017–7036; (b) J. M. Lehn, *Pure Appl. Chem.*, 1977, **49**, 857–870; (c) D. J. Cram and J. M. Cram, *Science*, 1984, **183**, 4127; (d) J. M. Lehn, *Angew. Chem., Int. Ed. Engl.*, 1988, **27**, 89–112.
- P. Guerriero, S. Tamburini and P. A. Vigato, *Coord. Chem. Rev.*, 1995, **110**, 17–243.
- (a) Q. Lu, J. J. Reibespens, A. E. Martell, R. I. Carroll and A. Clearfield, *Inorg. Chem.*, 1996, **35**, 7246–7252; (b) S. Aoki and E. Kimura, *J. Am. Chem. Soc.*, 2000, **122**, 4542–4548.
- N. M. Murthy, M. Mahroof-Tahir and K. D. Karlin, *Inorg. Chem.*, 2001, **40**, 628–635.
- C. Bazzicalupi, A. Bencini, A. Bianchi, V. Fusi, E. Garcia-España, C. Giorgi, J. M. Llinares, J. A. Ramirez and B. Valtancoli, *Inorg. Chem.*, 1999, **38**, 620–621, and references therein.
- (a) S. J. Lippard and J. M. Berg, *Principles of Bioinorganic Chemistry*, University Science Books, CA, 1994; (b) *Bioinorganic Catalysis*, ed. J. Reedijk, Dekker, New York, 1993.
- (a) K. D. Karlin, *Science*, 1993, **261**, 701; (b) D. E. Wilcox, *Chem. Rev.*, 1996, **96**, 2435–2458.
- M. N. Hughes, *The Inorganic Chemistry of the Biological Processes*, Wiley, New York, 1981.
- Y. L. Agnus, *Copper Coordination Chemistry: Biochemical and Inorganic Perspective*, Adenine Press, New York, 1983.
- (a) N. E. Dixon, C. Gazzola, R. L. Blakeley and B. Zerner, *J. Am. Chem. Soc.*, 1975, **97**, 4131–4133; (b) P. A. Karplus, M. A. Pearson and R. P. Hausinger, *Acc. Res. Chem.*, 1997, **30**, 330–337; (c) M. Musiani, E. Arnolfi, R. Casadio and S. Ciurli, *J. Biol. Inorg. Chem.*, 2001, **6**, 300–314.
- Zinc Enzymes*, ed. I. Bertini, C. Luchinat, W. Marek and M. Zeppezauer, Birkauser, Boston, MA, 1986.
- (a) C. J. Cooksey, P. J. Garratt, E. J. Land, S. Pavel, C. A. Ramsden, P. A. Riley and N. P. M. Smit, *J. Biol. Chem.*, 1997, **272**, 26226–26235; (b) L. M. Sayre and D. V. Nadkarni, *J. Am. Chem. Soc.*, 1994, **116**, 3157–3158; (c) A. Sánchez-Ferrer, J. N. Rodríguez-López, F. García-Cánovas and F. García-Carmona, *Biochim. Biophys. Acta*, 1995, **1247**, 1.
- (a) B. Linzen, N. M. Soeter, A. F. Riggs, H. J. Schneider, W. Schartau, M. D. Moore, E. Yokota, P. Q. Beherens, H. Nakashima, T. Takagi, T. Remoto, J. M. Vewreijken, H. J. Bak, J. J. Beintema, A. Volbeda and W. P. J. Gaykema, *Science*, 1985, **229**, 519.
- (a) P. Dapporto, M. Formica, V. Fusi, M. Micheloni, P. Paoli, R. Pontellini, P. Romani and P. Rossi, *Inorg. Chem.*, 2000, **39**, 2156–2163; (b) P. Dapporto, M. Formica, V. Fusi, M. Micheloni, P. Paoli, R. Pontellini and P. Rossi, *Inorg. Chem.*, 2000, **39**, 4663–4665; (c) N. Ceccanti, M. Formica, V. Fusi, L. Giorgi, M. Micheloni, R. Pardini, R. Pontellini and M. R. Tinè, *Inorg. Chim. Acta*, 2001, **321**, 153–161; (d) P. Dapporto, M. Formica, V. Fusi, L. Giorgi, M. Micheloni, P. Paoli, R. Pontellini and P. Rossi, *Inorg. Chem.*, 2001, **40**, 6186–6192; (e) M. Formica, L. Giorgi, V. Fusi, M. Micheloni and R. Pontellini, *Polyhedron*, 2002, **21**, 1351–1356; (f) M. Cangiotti, A. Cerasi, L. Chiarantini, M. Formica, V. Fusi, L. Giorgi and M. F. Ottaviani, *Bioconjugate Chem.*, 2003, **14**, 1165–1170.
- H. P. Berends and D. W. Stephen, *Inorg. Chem.*, 1987, **26**, 749.
- C. Bazzicalupi, A. Bencini, A. Bencini, A. Bianchi, F. Corona, V. Fusi, C. Giorgi, P. Paoli, P. Paoletti, B. Valtancoli and C. Zanchini, *Inorg. Chem.*, 1996, **35**, 5540–5548.
- F. H. Allen, *Acta Crystallogr., Sect. B*, 2002, **58**, 380–388.
- Copper Proteins, in *Metal Ions in Biology*, ed. T. Spiro, Wiley, New York, 1981, vol 3.
- P. Dapporto, M. Formica, V. Fusi, M. Micheloni, P. Paoli, R. Pontellini and P. Rossi, *Supramol. Chem.*, 2001, **13**, 369–377.
- P. Dapporto, V. Fusi, M. Micheloni, P. Palma, P. Paoli and R. Pontellini, *Inorg. Chim. Acta*, 1998, **275–276**, 168–174.
- M. Fontanelli and M. Micheloni, *1st Spanish-Italian Congress: Thermodynamics of Metal Complexes, Peñíscola, Spain, June 3–6, 1990*; University of Valencia, Valencia, Spain, 1990, p. 41.
- (a) G. Gran, *Analyst*, 1952, **77**, 661; (b) F. J. Rossotti and H. J. Rossotti, *J. Chem. Educ.*, 1965, **42**, 375–378.
- P. Gans, A. Sabatini and A. Vacca, *Talanta*, 1996, **43**, 1739–1753.
- N. Walker and D. D. Stuart, *Acta Crystallogr., Sect. A*, 1993, **39**, 158.
- SMART: Area-Detector Integration Software*, Siemens Industrial Automation, Inc., Madison, WI, 1995.
- SAINT Version 4.0*; Siemens Industrial Automation, Inc., Madison, WI, 1995.
- G. M. Sheldrick, *SADABS*, University of Göttingen, Germany, 1996.
- A. Altomare, G. L. Casciarano, C. Giacovazzo, A. Guagliardi, M. C. Burla, G. Polidori and M. Camalli, *J. Appl. Crystallogr.*, 1999, **32**, 115–119.
- G. M. Sheldrick *SHELX 97*, University of Göttingen, Germany, 1997.
- M. Nardelli, *Comput. Chem.*, 1983, **7**, 95–98.
- L. J. Farrugia, *J. Appl. Crystallogr.*, 1997, **30**, 565.